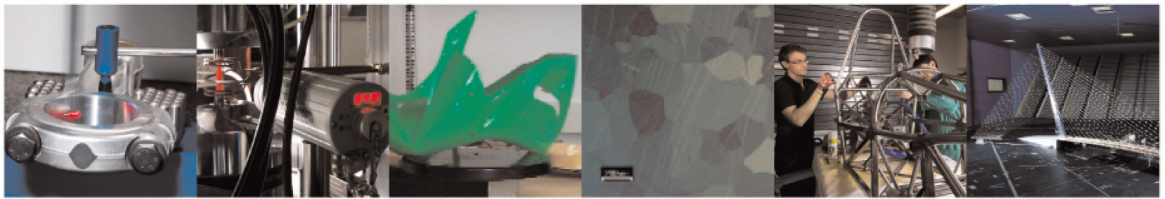




POLITECNICO
MILANO 1863

DIPARTIMENTO DI MECCANICA



Wearable biofeedback suit to promote and monitor aquatic exercises: a feasibility study

Gandolla Marta, Ferrante Simona, Costa Andrea, Bortolotti Dario,
Sorti Stefano, Vitale Federico, Bocciolone
Marco, Braghin Francesco, Masiero Stefano, Pedrocchi Alessandra

This is a post-peer-review, pre-copyedit version of an article published in IEEE TRANSACTIONS ON INSTRUMENTATION AND MEASUREMENT. The final authenticated version is available online at: <http://dx.doi.org/10.1109/TIM.2019.2911756>

© 2019 IEEE. Personal use of this material is permitted. Permission from IEEE must be obtained for all other uses, in any current or future media, including reprinting/republishing this material for advertising or promotional purposes, creating new collective works, for resale or redistribution to servers or lists, or reuse of any copyrighted component of this work in other works.

This content is provided under [CC BY-NC-ND 4.0](https://creativecommons.org/licenses/by-nc-nd/4.0/) license



Wearable biofeedback suit to promote and monitor aquatic exercises: a feasibility study

Gandolla Marta^{1*}, Ferrante Simona², Costa Andrea³, Bortolotti Dario², Sorti Stefano³, Vitale Federico^{4,5}, Bociolone Marco³, Braghin Francesco³, Masiero Stefano⁴, Pedrocchi Alessandra²

¹Nearlab@Lecco, Polo territoriale di Lecco, Politecnico di Milano, Lecco, Italy

²Nearlab, Dept. of Electronic, Information and Bioengineering, Politecnico di Milano, Milano, Italy

³Mechanical Dept., Politecnico di Milano, Milano, Italy

⁴Rehabilitation Unit, Department of Neuroscience, University of Padova, Padova, Italy

⁵Mare Termale Bolognese, Bologna, Italy.

Abstract — Aquatic exercises have been demonstrated to benefit the facilitation of motor recovery and the enhancement of well-being in middle-aged adults and the elderly. Personalization, immersiveness, and biofeedback are key for amplifying and accelerating any rehabilitation process in neurological and orthopedic patients. However, a therapist can neither properly visualize nor monitor rehabilitation exercises executed under water, nor can he/she measure them. Therefore, the present study aims to provide adaptive biofeedback during aquatic exercises in order to enhance the training's effectiveness. A wearable biofeedback suit equipped with wearable underwater-resistant sensor nodes has been designed, produced, and tested. A dedicated algorithm for quantitatively extracting joint angles has been developed and validated against the optical tracking system. Multiple biofeedback modalities are proposed based on visual feedback: amplitude control with set target angles; velocity-amplitude control with set target angles and angular velocity; and velocity tutor with set target angles, a frequency value, and a rest period. Joint angles estimated using the sensor network are compared to those estimated using an optical tracking system with the root-mean-squared angle error between the two systems ranging from 4.0° to 6.3° and a significant correlation coefficient that is always greater than 0.99. Pilot tests during aquatic exercises executed in a thermal environment demonstrate the feasibility and usability of the complete system in the final working environment. The relevant angles are

correctly calculated and monitored online during the exercises, and the tested subjects understand the implemented biofeedback modalities easily and follow them well as the SUS evaluation indicates.

I. INTRODUCTION

Aquatic rehabilitation or hydrokinesitherapy consists in body immersion (fully or partly) in water, combined with exercise therapy for medical purposes. Thanks to its physical properties, water represents an optimal environment for the mobilization of patients with musculoskeletal diseases. Furthermore, aquatic exercises proved to be beneficial in facilitating motor recovery and/or enhancing well-being in middle age adults and elders [1].

The main physical effects of immersion in water are related to temperature, buoyancy, viscosity, and hydrostatic pressure. Rehabilitation programs for patients with musculoskeletal disabilities take advantage of all these properties, since immersion: a) facilitates functional movement and improves the safety of exercises [2]; b) enhances the venous return of lower limbs [3]; c) helps relax muscles, reducing pain and muscular defense contracture, increasing joint range-of-motion, decreasing joint compression, weight load and muscular effort; d) provides higher resistance improving muscular tone, joint functionality and cardiovascular efficiency [4], which also benefit from the water cooling effect [5]. Moreover, coordination and balance are increased

during immersion, as water increases postural adjustment reactions. Last but not least, water immersion facilitates ambulation as it favors the upright stance and gait training [6]. From a technical point of view, movement in water requires motor strategies different from acquired and compensating automatisms. Outside water, human body kinetic schemes must continuously and primarily oppose gravity to generate movement; oftentimes, in muscle-skeletal disabilities these muscular synergies are altered, and patients cannot stand-up anymore make correct coordinated movements successfully. Exercise in water attenuates the antigravity component of muscular synergies and technically allows both the patient and the therapist to concentrate on the muscular group(s) and joint(s) specifically involved in the therapeutic exercise. In summary, water as a "rehabilitation tool" combines the advantages of immersion with the properties of therapeutic exercise.

As a result, the qualitative and quantitative measurement of movement in water would be of the utmost relevance in this field. In the absence of instrumental measurements, rehabilitation exercises performed in aquatic environments cannot be quantified, with at least two consequences: i) the therapist needs a close contact with the patient and an assiduous and often complex control for the real-time evaluation of the exercise; ii) since in principle the recovery effects achieved by aquatic rehabilitation should be subsequently confirmed outside water (results can in fact quickly disappear once back into gravity postural and motor conditions), there is no way to compare data during patient follow-up. The rehabilitation process would therefore greatly benefit from a continuous information flow and storage, quantitatively describing patients' real movements in water, let alone the obvious advantages of data storage and analysis for scientific purposes.

Currently available systems for technology-assisted rehabilitation often integrate some forms of visual and possibly multimodal feedback. Biofeedback is a technique that uses, for the purpose of motor learning, a backward external information (visual or auditory) transiently generated by a system capable of objectifying the performance [7]. The aim of rehabilitation biofeedback is to facilitate the

acquisition of sufficient control of the motor function by the patient and to obtain quantitative evaluation parameters for the therapist [5], [8]–[10]. Biofeedback, therefore, can improve accuracy during functional tasks, increase patient compliance and reduce the need for ongoing contact with healthcare professionals to monitor implementation of rehabilitation programs [11], [12].

The idea of associating biofeedback with hydrokinetic therapy requires the real-time capture and transmission of movement measures from the water. Underwater measurements have been of some interest when applied to performance monitoring in swimming. The most widespread approach to quantitatively investigate underwater movements is video-based with cameras positioned above and/or below the water [13]–[15]. Those systems are however cumbersome and time consuming, given that they foresee cameras placement underwater. Therefore, acquisitions have to be made in an instrumented pool, and the set-up is quite taxing. Moreover, data analysis algorithms are based on computer vision, which are computationally expensive, and the interaction with the system is quite difficult for non-technical users. A novel approach proposed in literature includes wearable inertial sensors (i.e., microelectromechanical systems, or MEMS, accelerometers and gyroscopes), which found it however hard to obtain accurate data in aquatic environments [16], as new technologies would be required. In addition, besides technical issues highlighted by Mooney and colleagues, the application filed for swimming presents differences in terms of quantitative variables of interest. To the best of our knowledge, there is a lack of studies on aquatic real-time movement measuring systems during rehabilitation.

The aim of this work is thus to conceive and design a system able to couple biofeedback with aquatic movement analysis based on multi-joint network of inertial sensors to enhance, personalize and objectify the in-water exercise.

Besides the aquatic environment, human movement tracking itself has been extensively investigated in the literature. Gold standard approach includes the use of motion capture systems with standardized [17] or ad-hoc [18] optical markers

placement, using either passive [19] or active [20] markers. However, optical motion capture systems and relative human motion tracking algorithms cannot be used in an aquatic context, for marker visibility issues, and due to optical distortion induced by water. The use of inertial sensors has been demonstrated to be versatile, reliable and low-cost in other motion tracking applications [21]–[25]. In the present context, indeed, versatility is a key requirement. The human body tracking system is intended to be able to track different combinations of body limbs (i.e., one or more legs, arms and spine, and potentially other human joints like neck or feet). These combinations need to be based on a minimal set of IMU. Therefore, in order to improve algorithm versatility depending on the number of sensors used, and the relative placement, Kalman Filter (or its variants) is not implemented in the whole process of sensor fusion and angle estimation given a model of the whole system, as [23], [25], but it is only used to reconstruct the coordinate system of each sensing node. The output of each Kalman Filter is a quaternion, to feed angle reconstruction, as in [24], [26]. It was in fact decided to acquire and process data using quaternions, which allows us, on the one hand, to improve computational efficiency, something crucial for real-time applications and, on the other hand, to avoid singularities [27], [28], especially in body motion estimation [11], [30]. Inertial-based human joint angle tracking has been already investigated in the literature (e.g., [23], [31]). However, a key aspect that is usually not addressed in motion tracking estimation using inertial sensors is the independence of the joints angle estimation from precise sensor placement. Indeed, in rehabilitation settings, the inertial units are managed and placed by a non-expert operator (i.e., therapist) on patient body segments, and precise sensors placement, therefore, should not be taken for granted. Absolute angular displacements of monitored body angles are nevertheless required, in order to relate the angles with actual motion. Typical solutions, based on extra sensors, such as magnetic sensors [21] or optical systems [29], are more expensive and less practical for our scope. In this view, we propose a solution, which requires the subject to assume certain calibration poses, a solution that does not involve anything but (possibly) external aids to reach the

required body displacement, and very little extra time.

The system should thus have the following characteristics: i) the sensor network should be flexibly mountable on multiple joints, allowing different configurations depending on user needs; ii) wearable biofeedback suit should be adaptable to different body sizes and easy to be donned and used, being the upper and lower part wearable separately or together; iii) the biofeedback provided should be kept as simple and understandable as possible, while providing enough information to be effective; iv) body angle tracking should be as independent from precise sensor positioning as possible. Different biofeedback modalities should be provided in order to comply with different needs. Both the user and the operator should receive a separate feedback with a differentiated content level; iv) recorded data should be saved, foreseeing the possibility to perform post-session data analysis; v) a complete report should be created for each session in order to build a user-specific database.

II. MATERIALS AND METHODS

A. Training Scenarios

Within the context of hydrokinesitherapy, three scenarios of exercises have been identified by the therapist personnel as representative of generic rehabilitation sessions. They cover the whole spectrum of classical possible exercises: one the whole body and two involving only its upper or lower parts respectively. In this way, one can monitor the general coordination of the user or portions of his/her body.

Thanks to a Graphical User Interface (GUI), the operator can select the training exercise, the biofeedback modality (whose options will be detailed in the following paragraphs) and several exercise parameters (e.g., exercises on range of motion, number of repetitions, exercise on difficulty, etc.) to tailor the exercise to the specific user with regard to training objectives.

Two illustrating training scenarios have been selected so to demonstrate the working principle throughout the whole manuscript (Figure 1). In particular, for the lower limb district, *hip*

flexion/extension (HFE) has been selected. The subject is instructed to flex and extend the hip, keeping the knee extended and the trunk still. The user can lean on a bar or on the poolside to sustain the body during the exercise. The hip ROM must not exceed 20° of extension and 80° in flexion so as not to request any trunk compensation. During the exercise, it is possible to use floats connected to the ankle, thus decreasing the concentric work and increasing the eccentric one. For the upper limb district, *shoulder abduction/adduction (SAA)* exercise has been selected. The user is standing or seated, with water up to the neck level. The initial pose of the forearm is anatomical. The shoulder must be abducted by 90°, not emerging from the water. A float around the wrist increases the difficulty.

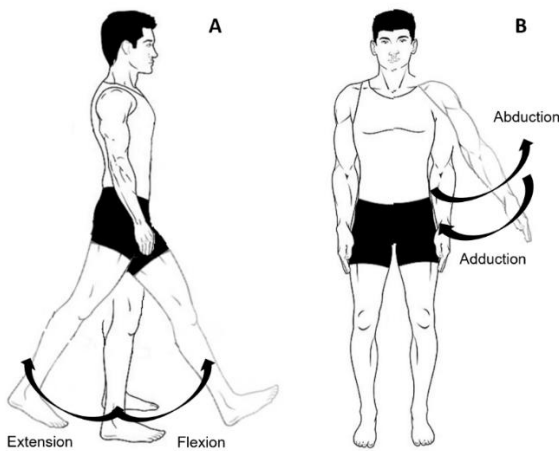


Figure 1. Training scenario graphical representation. A) hip flexion/extension (HFE); B) shoulder abduction/adduction (SAA).

B. System Description

The designed system consists of a wearable biofeedback suit equipped with a sensor network composed by several sensing nodes and a master node, which is able to transmit data in wireless mode to a receiving node placed outside the pool. The receiving node passes the data in quaternion form to a data processing unit (i.e., PC), which is in charge of data processing to obtain joint angle estimation. Joint angles are then passed to the biofeedback screen for real-time biofeedback to the user (Figure 2).

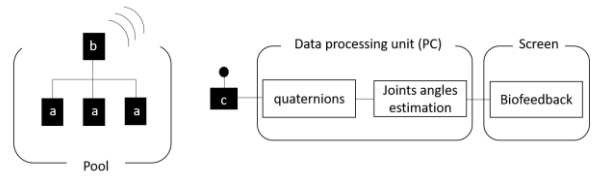


Figure 2. System overview. a: sensing node; b: master node; c: receiving node.

1) Wearable biofeedback suit

The suit has to support the developed sensor node network (Figure 3) to measure in-water movements, and it has to comply with both ergonomic and technical constraints. It must be easy to wear, it does not have to represent a constraint during exercises, and it should be adjustable both in length and in width to fit different body sizes.

The developed prototype consists of two different parts that can be worn independently, each one presenting housing slots to secure the sensing units. The top part includes a central section connected with two limb extensions. The abdominal wearability can be regulated by means of lateral and shoulder elastic straps. Both the arm and the forearm sections of the limb extensions can be regulated in width and secured with Velcro straps. The bottom part consists in a waist band connected with two limb extensions. All components can be regulated in width through Velcro straps. Lateral strips connecting the distal and the proximal section of each limb extension to the central section are used as accommodations for the wiring, improving the wearability and the freedom of movement. Sensing units are fastened onto the suit by means of a plug-and-socket connector sewed on the suit itself; no strict procedures are required for socket positioning with regard to the body. The surface of the whole prototype facing the user's skin is made of polychloroprene (Neoprene®), which adheres to the skin, limiting slipping during physical activity. As reported by the technical datasheet, the material guarantees that its shape is kept after repeated washing sessions for at least 2 years. Both the upper and the lower prototype parts are endowed with up to 5 sensing nodes (IMUs) each and one Master Node.

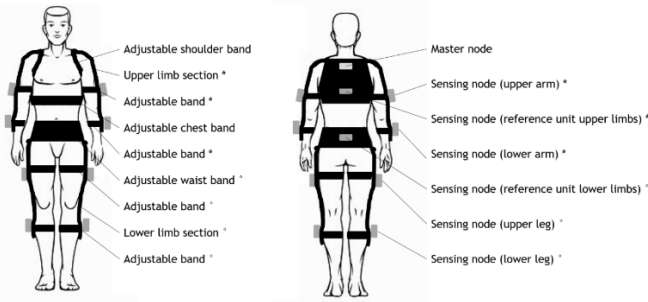


Figure 3. Wearable biofeedback suit concept. * Upper limb section; ° Lower limb section.

2) Sensor Network

The real-time monitoring sensor network was designed by considering power consumption as first driving optimization direction. Indeed, the system has to be suitable for use for at least a full rehabilitation session without the need to change/charge the sensors. A typical rehabilitation session lasts from 30 to 60 minutes. In this view, the network architecture proposed is low-power-oriented, in terms of both wireless communication and of electronics used in the hardware design. Focusing on the network architecture, many hardware/software protocols could be used (e.g., CAN, RS323, RS485, LIN), but it was decided to exploit the peripheral communication integrated in the inertial sensor and to create a digital bus line connecting the microcontroller and all the sensing nodes. The I2C interface was preferred over the SPI one, making it possible to design and handle the harness in a cleaner way using less signals. In this way, in the sensing nodes no microcontrollers or transceivers were used, reducing the current consumption of the whole system.

The designed real-time monitoring sensor network includes three components:

Sensing Nodes - each node embeds a triaxial 14-bit accelerometer, a triaxial 16-bit gyroscope, a triaxial geomagnetic sensor and a 32-bit cortex M0+ microcontroller, which provides I2C and SPI interface. In particular, each node includes a state-of-the-art IMU BNO055 (Bosch), which is typically designed for embedded applications, such as flight control and motion capture. BNO055 sensor combines Bosch's flagship 9 DoF motion sensor, the BMX055 (itself an agglomeration of the BMA055

accelerometer, BMI055 gyroscope, and BMM055 magnetometer), along with a ARM Cortex M0 processor. The sensor is equipped with a proprietary sensor fusion algorithm, which relies on an extended Kalman filter for the fusion proper, plus low and high-pass filtering, auto-calibration, and temperature compensation, in order to merge the three sensor data to be streamed into a quaternion representation of absolute orientation. The metrological characterization of the sensor has been recently investigated by Giancola and colleagues [32]. They successfully integrated the sensor in the integration of absolute orientation measurements in the Kinect fusion reconstruction pipeline.

The electronics is sealed in a waterproof case (30x50x10 mm) endowed with a plug-and-socket connector for anchoring it to the wearable biofeedback suit and a IP68 grade data connector used to communicate with the Master Node. A complete system includes a set of 5 Sensing Nodes, but any combination with less than 5 nodes can be used depending on physician needs.

Master Node - it gathers readings of up to 5 Sensing Nodes simultaneously and transmits them through low-power wireless (MiWi architecture, 0.9 GHz) to the receiver at a frequency of 20 Hz. In this view, the water paths will thus potentially affect data transmission only from master node to receiver node. It also endows the battery that powers the whole wearable sensing network.

Receiving Node - it acts as communication bridge between the Master Node and the Data Processing Unit (laptop PC) receiving the incoming data through low-power wireless.

C. Real time algorithm to extract relevant parameters from the sensor network

In order to estimate joint angles, it is necessary to measure the orientation of two adjacent body segments. In this work, upper limbs and lower limbs joint angles are alternatively measured, and in particular, for the upper limb case, shoulder and elbow angles are estimated, whereas for the lower limbs, hip and knee angles are calculated. The implied assumptions of the presented approach are: i) joints are modelled as spherical joints; ii) each sensor

is fixed in relation to its body segment (i.e., the relative motion due to muscles or fabric movement is neglected); iii) limbs and back are modeled as rigid segments.

When monitoring upper limbs, three sensors are used for each side, placed on the back (i.e., reference node - REF), on the upper arm (i.e., upper node - UN), and on the lower arm (i.e., lower node - LN), respectively. When monitoring lower limbs, the three sensors needed to monitor each side are placed on the pelvis (i.e., reference node - REF), on the thigh (i.e., upper node - UN), and on the shank (i.e., lower node - LN), respectively.

The sensors have to be placed on the corresponding segment, but it is not required that the positioning be repeatable between sessions. In order to define which of the active sensors is assigned to which body-segment, a manual identification is required for the operator through the GUI.

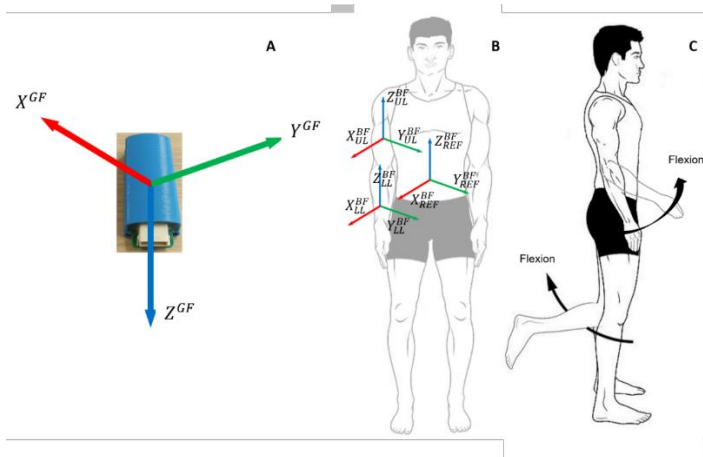


Figure 4. Real time algorithm to extract relevant parameters from the sensor network. A) sensor node reference frame, i.e., Global Reference Frame (GF) with Z-axis in the gravity direction, X-axis in the Earth Magnetic North Pole direction, and the Y-axis derived to form a right-handed system. B) Body reference frames (BF) placed on respective body segments with the Z-axis longitudinal to the main dimension of the segment itself, the X-axis frontally outgoing from the body segments, and the Y-axis derived to form a right-handed system. C) Demonstration of movements required in the dynamic calibration step, i.e., elbow flexion (when monitoring upper limb exercises) or knee flexion (when monitoring lower limb exercises).

1) Sensor reference frames and body segment reference frames

Each sensor provides data in quaternion form in respect of a Global Reference Frame (GF) with Z-axis (i.e., Z^{GF}) in the gravity direction, X-axis (i.e., X^{GF}) in the Earth Magnetic North Pole direction, and the Y-axis (i.e., Y^{GF}) derived to form a right-handed system (Figure 4, panel A). Subscript codes indicate the node position on the subject, e.g., X_{UN}^{GF} refers to the X-axis in the global reference frame for the upper limb node. The output quaternion from each sensor node is indicated as $q_{t,i}^{sens,GF}$, where t,i indicates the sample t acquired by the node i , which represents the IMU placement on the subject (i.e., $i = REF; UN; LN$), and $sens,GF$ indicates that the quaternion describes the position of the sensor ($sens$) in the global reference frame (GF).

For each body segment, a dedicated Body Frame (BF) reference system has been defined with the Z-axis (i.e., Z^{BF}) longitudinal to the main dimension of the segment itself, the X-axis (i.e., X^{BF}) frontally outgoing from the body segments, and the Y-axis (i.e., Y^{BF}) derived to form a right-handed system (Figure 4, panel B). Again, subscript codes indicate the node position on the subject, e.g., X_{UN}^{BF} refers to the X-axis in the body reference frame for the upper limb node.

2) Calibration procedure

For an accurate angle estimation [33], a calibration procedure has been implemented so to define the mapping of the reference system of each sensor node (i.e., GF reference systems) to the corresponding body frame reference system (i.e., BF reference system). Given that with regard to the aforementioned hypothesis each sensor is modeled as fixed compared to its body segment, the calibration procedure has to be performed once for all. The calibration procedure is performed in two steps: a) static calibration step, and b) dynamic calibration step.

Static calibration step – The aim of this procedure is to map Z^{GF} axis on Z^{BF} axis. The user, wearing the desired sensing network setup, assumes the static calibration position, i.e., straight legs and arms in line with the trunk (Figure 4, panel B). The operator shall

assess the correct posture before starting the static calibration routine. The static calibration position has by hypothesis all Z_i^{BF} axes oriented vertically, as shown in Figure 4, panel B. The relative position of Z^{GF} axis compared to Z^{BF} axis described in quaternion form is calculated as (1):

$$\text{conj}(q_{0,i}^{BF,GF}) \times q_{0,i}^{\text{sens},BF} = Q_{0,i}^{\text{sens},BF} \quad (1)$$

where subscript 0,i indicates position at time 0 (i.e., calibration position) for each of the existing nodes; sens,GF indicates the quaternion describing the position of the sensor (sens) in the global reference frame (GF); BF,GF indicates the quaternion describing the position of Z^{BF} axis in the global reference frame (GF), which is taken as vertical as previously discussed; and sens,BF indicates the quaternion describing the position of the sensor (sens) in the body reference frame (BF). To reject small unwanted body motions while keeping the position, $q_{0,i}^{\text{sens},GF}$ signals are acquired over 2 seconds and averaged.

Given that each sensor is modeled as fixed with respect to its body segment, the following equation holds for any acquired sample, i.e., for any given t (2):

$$\text{conj}(q_{0,i}^{\text{sens},BF}) = \text{conj}(q_{t,i}^{\text{sens},BF}) \quad (2)$$

At this point, quaternion $q_{0,i}^{\text{sens},BF}$ describes the relative position between the body segment reference frames, and the sensor global reference frames, only in respect of Z-axis orientations.

Dynamic calibration step – The aim of this procedure is to determine the X^{GF} orientation as regards X^{BF} , hypothesized as normal to the user’s chest (Figure 4, panel B), so as to fully characterize the relative position between the body segment reference frames and the sensor global reference frames. The operator shall lead the user to form a small angle ($\sim 20^\circ$) keeping the proximal segment (i.e., upper arm or thigh) vertical and lifting the distal (i.e., lower arm or shank) parallel to the sagittal plane (Figure 4, panel C). Distal segment pointing direction (projected onto ground plane) is an acceptable approximation for normal of the chest. The projection of the distal segment’s Z-axis (Z_{LN}^{BF}) onto the X^{GF} - Y^{GF} plane is calculated (i.e., $Z_{LN,proj}^{BF}$), and the angular offset between $Z_{LN,proj}^{BF}$ and X^{GF} is then

computed in order to define the relative orientation between BF and GF providing a fully defined identification of body frames ($q_{0,i}^{BF,GF}$).

3) Joints angle real-time calculation

The quaternion describing the position of each body segment at time point t is described by the following equation (3):

$$q_{t,i}^{BF,GF} = q_{t,i}^{\text{sens},GF} \times \text{conj}(q_{0,i}^{\text{sens},BF}), \quad (3)$$

where $q_{t,i}^{\text{sens},GF}$ are data coming from the sensor node i; $q_{0,i}^{\text{sens},BF}$ is the result of the calibration procedure describing the relative position of the sensor on the body frame; and $q_{t,i}^{BF,GF}$ is the quaternion describing the motion of the body segment in the body segment reference frame. Body segment angles are then calculated following the International Society of Biomechanics (ISB) convention [27], [28]. To that end, the Direction Cosine Matrix (DCM) is calculated as follows (4):

$$DCM = \begin{bmatrix} q_0^2 + q_1^2 - q_2^2 - q_3^2 & 2(q_1q_2 + q_0q_3) & 2(q_1q_3 - q_0q_2) \\ 2(q_1q_2 - q_0q_3) & q_0^2 - q_1^2 + q_2^2 - q_3^2 & 2(q_2q_3 + q_0q_1) \\ 2(q_1q_3 + q_0q_2) & 2(q_2q_3 - q_0q_1) & q_0^2 - q_1^2 - q_2^2 + q_3^2 \end{bmatrix} \quad (4)$$

being $q_{t,i}^{BF,GF} = (q_0, q_1, q_2, q_3)$. Each column of the DCM is one axis of the body segment tracked i (i.e., \bar{X}_i^{BF} , \bar{Y}_i^{BF} and \bar{Z}_i^{BF} , respectively).

Bearing in mind that the relative angle between two vectors is performed according to (5):

$$\alpha(A, B) = \text{atan2} \left(\frac{\|A \times B\|}{A \cdot B} \right) \quad (5)$$

main upper limb angles are thus identified and calculated as shown in Table 1 [31].

Joint	Angle	Equation
Shoulder/hip	plane of elevation angle	α_{UN} = $\alpha(\bar{X}_{REF}^{BF}, \bar{Z}_{UN}^{BF})$ $\bar{Z}_{UL}^{BF} = \bar{Z}_{UN}^{BF}$ projection onto transverse plane
Shoulder/hip	elevation angle	β_{UN} = $\alpha(\bar{Z}_{REF}^{BF}, \bar{Z}_{UN}^{BF})$
Shoulder/hip	internal/external rotation	$\gamma_{UN} = \bar{Z}_{UN}^{BF}$
Elbow/knee	flexion/extension	β_{LN} = $\alpha(\bar{Z}_{UN}^{BF}, \bar{Z}_{LN}^{BF})$
Elbow/knee	internal/external rotation	$\gamma_{LN} = \bar{Z}_{LN}^{BF}$

Table 1. Upper limb angles equations, as implemented in the present work.

D. Biofeedback Solution

The provided biofeedback solution has two different interfaces: one for the user to increase awareness of its body position and movements (i.e., user biofeedback interface), and one for the operator to monitor the ongoing session (i.e., operator monitoring interface).

1) User Biofeedback Interface

One of the main goals designing a device that needs to be interfaced also with users (who can be patients or elders) as well is to be able to provide an output as comprehensible and simple as possible while still maintaining a sufficient level of information content. Considering that, most likely, during the in-water therapy the user will not be able to use hearing aids and glasses, the essential visual outputs have been selected to be exclusively pictographic and well-readable numbers.

The user interface consists of two stylized human figures representing the initial and final task positions and a cursor linked to the joint angle selected to be representative of the exercise, e.g., shoulder elevation in the frontal plane (Figure 5, panel A). On the upper right corner, the actual number of repetitions over the total required is indicated. A visual feedback is given to the user depending on his/her position (Figure 5, panel A): different background colors warn the user when approaching the targets (neighborhood areas - Yellow background), in the proximity of the targets (target areas - Green background) or after overstepping the targets (external invalid areas - Red background). An additional angle can be monitored (Secondary Monitored Angle) and linked to the biofeedback resulting in a red exclamation mark prompt whenever the correspondent threshold is exceeded. For example, during SAA exercise, the elbow should remain extended. In this case, elbow angle can be selected as secondary monitored angle. In other words, when the user flexes the elbow exceeding an operator-defined threshold, the red exclamation mark shows up, reminding the user to keep the elbow extended (Figure 5, panel B).

Three biofeedback modalities have been designed, in particular:

Amplitude control biofeedback – the user is required to perform an angular excursion previously defined by the operator at a self-paced velocity (Figure 5 panels A, B). The user can stop at any time.

Amplitude/velocity control biofeedback - the user is required to perform an angular excursion previously defined by the operator at a defined velocity. A negative feedback (Red iconized turtle, Figure 5, panel C) is provided when the motion speed is lower than the required one.

Tutor biofeedback - the user is required to perform an angular excursion previously defined by the operator at a defined velocity following a virtual tutor. In the exercise progression bar, beside the cursor linked to the articular angle chosen to be representative of the exercise (e.g. shoulder elevation on the frontal plane for the SAA exercise), a second red cursor is shown, representing the desired joint position (Figure 5, panel D). A green-yellow-red color code for the angular excursion bar is adopted for the bar to alert the user as the absolute distance between the two pointers increases. After performing one complete movement, the user is asked by a countdown to wait in a resting position before proceeding with the new repetition.

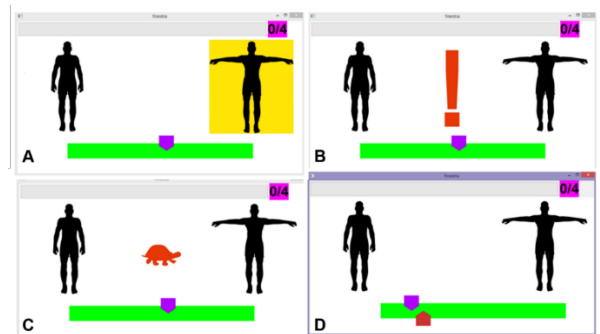


Figure 5. Examples of user interface. A) user interface with the two stylized human figures representing the initial and final task positions and the cursor linked to the joint angle selected to be representative of the exercise with visual feedback for the user approaching the target (i.e., yellow background); B) Secondary Monitored Angle feedback; C) velocity feedback; D) tutor biofeedback interface.

2) Operator monitoring interface

Through the operator biofeedback interface, the operator selects which angles to monitor in real time (affecting the operator interface only).

	Amplitude control	Amplitude/velocity control	Tutor
SAA	Abduction Target	Abduction Target	Abduction Target
	Adduction Target	Adduction Target	Adduction Target
	Repetition Number	Repetition Number	Repetition Number
	Difficulty	Difficulty	Difficulty
	Additional Parameter Binding	Additional Parameter Binding	Additional Parameter Binding
	Exercise Side	Exercise Side	Exercise Side
	Minimum Velocity	Minimum Velocity	Minimum Velocity
	Rest Time	Rest Time	Rest Time
HFE	Flexion Target	Flexion Target	Flexion Target
	Extension Target	Extension Target	Extension Target
	Repetition Number	Repetition Number	Repetition Number
	Difficulty	Difficulty	Difficulty
	Additional Parameter Binding	Additional Parameter Binding	Additional Parameter Binding
	Exercise Side	Exercise Side	Exercise Side
	Minimum Velocity	Minimum Velocity	Minimum Velocity
	Rest Time	Rest Time	Rest Time

Table 2. Complete list of modifiable parameters. Difficulty: three difficulty levels (i.e., easy, medium, hard) determine the tolerance toward user errors. Additional parameter binding: this option allows us to provide the user with an additional visual feedback correlated with the secondary monitored angle. Exercise Side: when a complete upper or lower body network is used, the operator must select which side to monitor. Minimum Velocity: the slowest movement speed accepted [%/sec] during the exercise execution. Slower movements will trigger a visual feedback (except during changes of direction). Repetition Time: time taken by the Tutor's cursor to perform a single repetition. Rest Time: resting time between repetitions.

Joint angles	Minimal Required Network
Shoulder Elevation	3 + 4 + (9 or 10) + MN or 7 + 8 + (9 or 10) + MN
Shoulder Plane of Elevation	3 + 4 + (9 or 10) + MN or 7 + 8 + (9 or 10) + MN
Elbow Flexion-Extension	3 + 4 + (9 or 10) + MN or 7 + 8 + (9 or 10) + MN
Hip Frontal	1 + 2 + (9 or 10) + MN or 5 + 6 + (9 or 10) + MN
Hip Sagittal	1 + 2 + (9 or 10) + MN or 5 + 6 + (9 or 10) + MN
Knee Flexion-Extension	1 + 2 + (9 or 10) + MN or 5 + 6 + (9 or 10) + MN
Torso Flexion-Extension	9 + 10 + MN
Torso Side Bending	9 + 10 + MN
Torso Rotation	9 + 10 + MN

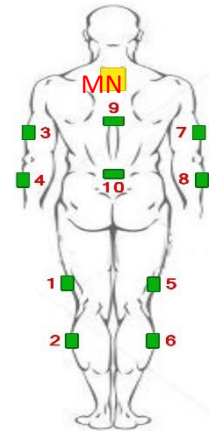


Table 3. Minimal required network to be able to monitor the selectable angles. MN: Master Node.

Personalization – Depending on the selected combination between exercise and biofeedback modality, the operator can alter various settings as reported in Table 2.

Online monitoring - The operator can select two additional angles to be monitored (other than the one directly related to the selected exercise) among the following: Shoulder Elevation, Shoulder Plane of Elevation, Elbow Flexion-Extension, Hip Frontal, Hip Sagittal, Knee Flexion-Extension, Torso Flexion-Extension, Torso Side Bending, Torso Rotation. The selection must agree with the sensor network setup, as indicated in Table 3. Each angle is paired with an angular threshold agreed beforehand with the physicians. Where allowed (see Table 2, “Additional parameter binding”), the operator can activate an additional visual feedback on the user biofeedback interface bound with one of the two

additional selected angles (exclamation mark in Figure 5, panel C).

3) Score and report

Once the biofeedback is started, the user will be asked to repeat a certain movement for a defined number of times. A repetition is defined as two subsequent changes in direction. A custom-made algorithm is used to analyze real-time angular data to evaluate the user performances at the end of the exercises session(s).

At the end of each exercise, recorded data are saved under quaternion form to be processed to perform further offline analysis. These data can be used to generate a Single Session Report or a Multiple Session Report. The single session report presents all the settings used to perform the selected exercise and the Score obtained and shows the time profile among all repetitions of the parameters of interest with relative thresholds. The multiple sessions report gathers the final output (Score or Step velocity) of all the records (from the same user) that share the same exercise type, and provides a performance trend.

E. System Validation

1) Metrological characterisation

To characterize the designed acquisition setting, which includes sensors and the developed algorithm, the uncertainty of the system under static conditions was investigated following the Guide to the Expression of Uncertainty in Measurement [34]. A 5-DoF upper limb exoskeleton was used, made up of 5 stepper motors (2xST4118 and 3xST2818, Nanotech) controlled by dedicated drivers (SMCI33, Nanotech). Motor positions are monitored by an optical encoder (WEDS series, Nanotech). The robotic arm used has an angular resolution of 0.02° , with an associated estimated uncertainty of 0.006° , which is therefore negligible compared to expected IMU uncertainty [32]. The reference sensing node was placed at the shoulder level, the upper arm sensing unit on the link between the shoulder and the elbow joints, and the lower arm sensing unit on the link between the elbow and the wrist. As seen in the literature [32], the robotic arm was used to move the elbow in steps of 5° within the whole range of motion ($0-140^\circ$). For

each angle, after a stabilization of 5 s, 1000 samples were measured by our IMU-based system, and calculated by the developed algorithm as the angle between the upper arm sensing unit and the reference sensing unit, at a frequency of 20Hz. Uncertainty was measured as a combination of a random error represented by the standard deviation of the error between the two acquisition systems and a systematic error measured by the means of the error between the two acquisition systems.

2) Real time algorithm validation

Two shoulder movements have been selected to validate the developed algorithm, in particular i) shoulder abduction/adduction, and ii) shoulder flexion/extension. To validate the developed algorithm, the angles at shoulder level have been simultaneously recorded both by the sensing nodes and by an optical tracking system with six cameras (Smart DX400, BTS Bioengineering).

Experimental protocol - For each selected movement (i.e., i) shoulder abduction/adduction, and ii) shoulder flexion/extension), 3 separate runs with 10 movement repetitions were performed for a total of 30 shoulder abduction/adduction, and 30 shoulder flexion/extension movements. The subject was required to execute the two protocols starting from an upright position, i.e., straight legs and arms in line with the trunk (Figure 6, panel B), abducting/flexing the shoulder up to 90° and going back to the upright position. The three runs have been performed with a 30 minutes' interval with no data acquisition to account for possible sensor drift.

Optical tracking system measures and analysis - Twelve passive retro-reflective markers have been placed on a healthy volunteer (who signed an Informed Consent). In particular, 3 triplets arranged as orthogonal reference frames have been fastened onto the three sensing nodes placed respectively on the trunk, arm, and forearm, while three further markers have been placed on acromion, elbow, and wrist (Figure 6, panel A, B). The sampling frequency was set at 120 Hz. Marker trajectories were analysed with a custom algorithm running in Matlab. Trajectories from all markers were interpolated with cubic splines to reconstruct the possible missing kinematic data and filtered with a second-order

Butterworth low-pass filter (cut-off frequency = 1 Hz). Markers placed on acromion, elbow and wrist were used to track upper and lower arm position, as the segment from the acromion to the elbow, and from the elbow to the wrist respectively. The three triads are processed in the same way as the sensor network quaternions to obtain joint angles, i.e. they are considered as fixed on body segments and used to track it (Figure 6, panel C).

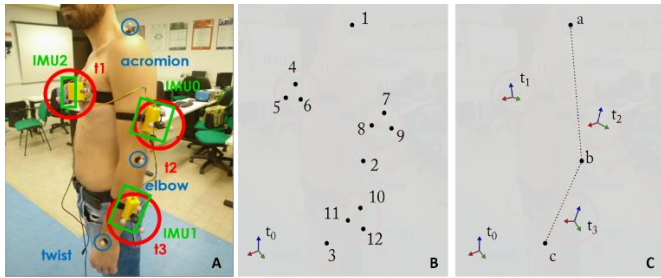


Figure 6. A) Experimental set-up on the subject for system validation, comparing the angular estimation obtained with the developed algorithm with the one measured by an optical system. B) Optical markers placement. 1: acromion; 2: elbow; 3: wrist; 4-6: triplet arranged as orthogonal reference placed on the trunk sensing node; 7-9: triplet arranged as orthogonal reference placed on the arm sensing node; 10-12: triplet arranged as orthogonal reference placed on the forearm sensing node. C) Upper and lower arm identification. a: Acromion; b) elbow; c) wrist; segment a-b: upper arm; segment b-c: lower arm; t1-t3: triad identification superimposed to sensors.

Measurement comparison - The measurement revealed by the two experimental set-ups (i.e., sensor network and optical tracking system) have been compared by means of the correlation coefficient r and the root mean squared error (RMSE) between the shoulder angles measured during the three runs for both selected movements, i.e., i) shoulder abduction/adduction, and ii) shoulder flexion/extension. Based on the literature, a correlation coefficient of 0.95 and a RMSE less than 8° have been set as the validation threshold [35].

3) In water validation

The ability of the sensor network to collect data when the sensing nodes are submerged has been tested before to proceed to test the system in aquatic

(thermal) environment. The experimental set-up is shown in Figure 7. An L-shaped support equipped with an L-shaped passive one degree of freedom serial arm has been placed in an empty bucket. The passive serial arm has been connected to the end effector of a NAO robot by means of a thread so that the NAO end effector was able to move the L-shaped passive arm along its degree of freedom. Two sensing nodes have been placed on the two arms of the passive arm, and a third sensing node (i.e., reference sensing node) has been placed on the L-shaped support. The master node was placed on the table close to the NAO robot.

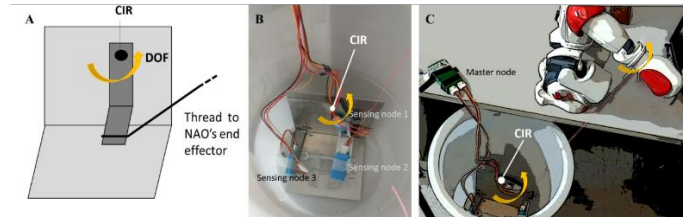


Figure 7. Experimental setup for in water validation. A) drawing of the L-shaped support and the one degree of freedom passive arm; B) sensing nodes placement; C) complete experimental set-up. CIR = Center of Rotation.

Experimental protocol - The NAO's end effector was programmed to cyclically reach an angular position of 90 degrees and keep it for 3 seconds. Both systems (i.e. sensor network and NAO) recorded their angular position for offline analysis. The same test was performed by immersing the passive arm (and sensing nodes) in salty water (1.5g/l of NaCl). 10 cycles per condition (in water, outside water) were recorded from both sensor network and NAO system.

Measurement comparison - The goal of in-water validation is to compare data collected from the sensor network in the dry and wet conditions. To that end, the angular position of the passive arm has been calculated with the developed algorithm where sensing nodes 1 and 2 were considered as placed on the upper and lower arm respectively, and sensing node 3 was considered as the reference node. The angle of the passive arm has been calculated as the angle at shoulder level. The angular measurement detected in the two experimental conditions (i.e., dry and wet) have been compared by means of the correlation coefficient r and the root mean squared

error (RMSE) between the mean angles measured during the 10 repeated movements.

4) Pilot tests in aquatic (thermal) environment

Shoulder abduction/adduction training scenario has been selected as representative exercise to be tested as aquatic exercises with the three biofeedback solutions developed. The wearable biofeedback suit prototype has been worn with three sensing units placed on the trunk, the upper arm, and the lower arm, respectively. A screen has been placed on the swimming pool edge to show the biofeedback (Figure 8). Two healthy volunteers (S01: f, 20 years old; S02: m, 20 years old) tested the system.

The subjects were instructed to perform 3 runs: i) 10 movements with amplitude control feedback; ii) 10 movements with amplitude/velocity control feedback; iii) 10 movements with tutor control feedback. During the different runs, the subjects were instructed to make errors on purpose to test biofeedback usability, and the number of lost data packages was recorded. At the end of the test, the users were then required to score the system on the base of the System Usability Scale - SUS [36].



Figure 8. Experimental set-up for pilot tests in aquatic thermal environment. The user interface is displayed on the screen during the exercise. Other examples of user interface are shown in Figure 5.

III. RESULTS

A. Metrological characterisation

Measurement uncertainty presents a systematic error within 5° , but negligible random error (Figure 9, panels A-B). The systematic error is mainly due to the calibration between the two sensing units, and to possible reference unit motion.

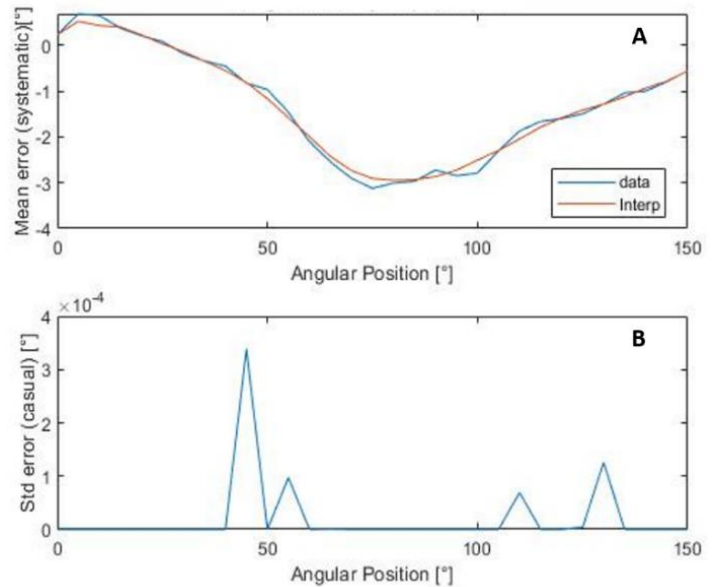


Figure 9. Metrological characterization of the systematic (A) and random (B) errors obtained on the angle measured by the proposed system against the robotic arm used as gold standard.

B. Real-time algorithm validation

During the experimental sessions, the mounting of the IMUs to certain locations or orientations was not restricted. Calibration duration was always less than 15 seconds. Joint angles at shoulder level were calculated for the two experimental set-ups (i.e., sensor network and optical tracking system). A representative example for both experimental conditions is shown in Figure 10. The correlation coefficient r and the root mean squared error (RMSE) between the shoulder angles measured during the three runs is shown in Table 4. Overall, the mean correlation coefficients proved to be 0.992 and 0.994 for shoulder abduction/adduction and shoulder flexion/extension, respectively, both higher than the set threshold (i.e., 0.95). Similarly, mean RMSE for both selected exercises proved to be below the set threshold, more specifically, 4.7° and 5.6° for shoulder abduction/adduction and shoulder flexion/extension, respectively.

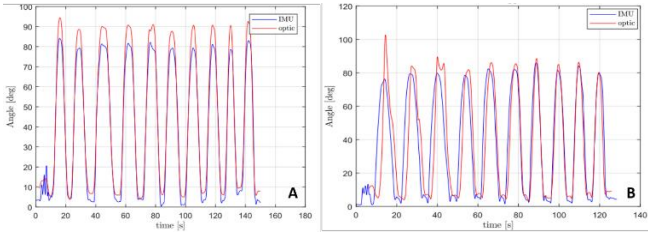


Figure 10. Visual comparison of shoulder angles measured by the sensor network (blue lines) and optical tracking systems (red lines) during (A) Shoulder Abduction-Adduction, and (B) Shoulder Flexion-extension.

Task	Run 1		Run 2		Run 3		Mean	
	R		R		R		R	
	<i>r</i>	M SE (°)	<i>r</i>	M SE (°)	<i>r</i>	M SE (°)	<i>r</i>	M SE (°)
Shoulder abduction/adduction	0.99	4.0	0.99	4.4	0.99	5.5	0.99	4.7
Shoulder flexion/extension	0.99	4.6	0.99	5.7	0.99	6.3	0.99	5.6
	2	1	1	1	1	1	1	1
	3	3	3	6	4	4	4	4

Table 4. Correlation coefficient *r* and root mean squared error (RMSE) between the shoulder angles measured during the three runs.

C. In water validation

Passive serial arm angles were calculated for the two experimental conditions (i.e., dry and wet conditions). The correlation coefficient between the mean angle profile obtained during the 10 repetitions for both conditions is 0.998 with associated *p*-value < 0.001. RMSE proved to be equal to 1.9°. We can therefore conclude that the two experimental conditions are comparable.

D. Pilot tests in aquatic (thermal) environment

The volunteers successfully tested the system in the aquatic thermal environment. The master node correctly sent data coming from the sensing nodes, and the biofeedback interface was correctly running. A brief video showing the effective session is shown in the video included as Supplementary Material.

SUS evaluation was 85%, for both S01 and S02. All packages were successfully acquired during all runs.

IV. DISCUSSION

It is now well established that therapeutic aquatic exercise has many application areas in rehabilitation. Here we described a wearable biofeedback suit prototype - unique in its kind - able to quantitatively measure aquatic patient movements, transferring data outside water for biofeedback generation, and data storage for subsequent analysis. The idea has been submitted for patent purposes (issue number 10201800006950, submitted on 2018/07/05 at the Italian patent office). The wearable biofeedback suit prototype consists of an adjustable upper/lower limbs part that meets an easy to wear requirement, adjustable in size, and hygienic (i.e., it can be easily washed if needed). The wearable biofeedback suit has plastic cases to host the sensor network. A reference sensor node, and at least two sensor units, have to be placed on the wearable biofeedback suit in order to track joint angles. Indeed, the developed wearable biofeedback suit needs to be improved in terms of design, lavishing special care on the inclusion of the cables in the suit itself so that they do not accidentally interfere with movements, especially for severely impaired patients. Throughout the manuscript, two illustrating exercises were shown and described in detail. It should be noted, however, that technology can be easily implemented to allow the production of biofeedback exercise settings for any body district, depending on specific needs.

A master node is sealed inside its case and placed right below the subject's neck. In fact, data is transmitted from the master node to the receiving node through low-power wireless, being waterproof sensors and cables. We noticed that up to 10 cm underwater signal attenuation is acceptable in thermal water. In this view, we thought that wireless communication was acceptable for the master node that, being attached to the subject's upper back, will likely be submerged for no more than 10 cm in depth during its real use in rehabilitation. When submerged more deeply, the transmission pauses, resulting in a local data loss. Once the optimal positioning is restored, the data stream resumes automatically. As a consequence, the sensing nodes attached for example

to legs are not suitable for wireless communication. The innovative contribution of this approach, therefore, is not linked to underwater data communication in itself: no available system provides a waterproof device that sends and processes in real-time inertial data from a human motion capture system. As far as we know, current solutions employed in underwater applications store data for subsequent analysis [16].

The wearable biofeedback suit prototype is equipped with a screen to be placed on the pool edge to show the biofeedback during training. Three biofeedback modalities have been designed so to fulfil different needs, i.e., amplitude control, amplitude/velocity control, and tutor.

Joint angles measured during wearable biofeedback suit use proved to be reliable in dry and wet conditions. Quaternions are processed in real time, and joint angles are coherently extracted. The developed algorithm was based on previous works [31], introducing however the further degree of freedom given by the fact that the sensors just need to be placed on the corresponding segment, but their exact anatomical positioning is not a mandatory requirement to obtain repeatable data between sessions. This is a key aspect for the effective use of human motion tracking systems in a clinical context where technologies are used by non-expert operators.

Joint angles estimated by the sensor network were compared to those estimated by an optical tracking system. The two independent systems are calibrated to be coherent in coordinate systems, as previously introduced in sensor fusion approaches [30], and their data is processed with the same mathematical steps. RMS angle error between the two systems ranged from 4.0° to 6.3° , with a significant correlation coefficient always higher than 0.990. This is a very reasonable error if compared to what has been achieved in the literature - 4.4° to 6.5° [35] and 12° – 16° [37]. Angular excursion of a passive serial arm has been monitored in dry and wet conditions. Although acquired in two different runs, measured angles proved to be comparable with a RMSE of about 2° , well below the set validation threshold (i.e., 8°). Pilot tests in aquatic thermal environment demonstrated the feasibility and usability of the complete system in a final working environment.

The applications of this system potentially range from rehabilitation to athletic training and research in the field of aquatic kinematics. Given that biofeedback allows faster and more effective recovery, with a pronounced proprioceptive nuance, the applications of wearable biofeedback suit in human rehabilitation can be envisaged in: orthopedic and rheumatic diseases [38], accompanied by general symptomatology - subacute and chronic pain syndromes, reduction of ROM, post-lesion recovery of soft tissue or bone and postoperative recovery [39]; scoliosis and pain management, especially in back pain; sports traumatology and spine trauma. With neurological diseases - where both biofeedback and the microgravity condition of water immersion (which allows movement even in the presence of significant deficits of motor units recruitment) find precise indications, wearable biofeedback suit would, for example, allow biofeedback-assisted aquatic step training in post-stroke [40] and hemiplegic patients [41], in para and tetraplegia and in Parkinson's disease [42], [43]. Patients whose residual motor capacities do not allow “dry” rehabilitation programs lose the potential advantages of biofeedback. Instead (provided that potential accompanying cognitive deficits allow the patient to keep the attention for the time needed for exercises), biofeedback-driven aquatic movements would allow stimulation of patients' residual cognitive functions (i.e. for the dyspraxic patient, wearable biofeedback suit might be ineffective). Finally, thanks to its motion analysis features, the wearable biofeedback suit prototype might be used for prevention, allowing the clinician to anticipate the detection of changes in the pathological conditions.

To sum up, it a complete set-up suitable for underwater real-time human motion tracking has been presented, along with on-line multiple biofeedback modalities for the user executing the exercise. A wearable biofeedback suit equipped with wearable underwater resistant sensor nodes has been designed, produced and tested, including a dedicated algorithm to quantitatively extract joints angles, which has been developed and validated with a metrological characterization, and against the optical tracking system. Pilot tests during aquatic exercises executed in thermal environment demonstrated the feasibility and usability of the complete system in the

relevant working environment with recorded good system usability evaluation.

V. ACKNOWLEDGEMENTS

The presented work was supported by “Fondazione per la ricerca scientifica termale” grants.

References

- [1] J. Kisner, C., Colby, L. A., & Borstad, *Therapeutic exercise: foundations and techniques*. 2017.
- [2] Y. Alikhajeh, S. R. A. Hosseini, and A. Moghaddam, “Effects of Hydrotherapy in Static and Dynamic Balance Among Elderly Men,” *Procedia - Soc. Behav. Sci.*, vol. 46, pp. 2220–2224, Jan. 2012.
- [3] E. Watanabe, N. Takeshima, A. Okada, and K. Inomata, “Comparison of water- and land-based exercise in the reduction of state anxiety among older adults.,” *Percept. Mot. Skills*, vol. 91, no. 1, pp. 97–104, Aug. 2000.
- [4] C. Konlian, “Aquatic therapy: making a wave in the treatment of low back injuries.,” *Orthop. Nurs.*, vol. 18, no. 1, pp. 11-8; quiz 19-20.
- [5] J. P. S. Becker Bruce E., Kasee Hildenbrand, Rebekah K. Whitcomb, “Biophysiologic Effects of Warm Water Immersion,” *Int. J. Aquat. Res. Educ.*, vol. 3, pp. 324–37, 2009.
- [6] S. Masiero, “Thermal rehabilitation and osteoarticular diseases of the elderly.,” *Aging Clin. Exp. Res.*, vol. 20, no. 3, pp. 189–194, Jun. 2008.
- [7] J. A. Onate, K. M. Guskiewicz, and R. J. Sullivan, “Augmented Feedback Reduces Jump Landing Forces,” *J. Orthop. Sports Phys. Ther.*, vol. 31, no. 9, pp. 511–517, Sep. 2001.
- [8] G. Tacchino, M. Gandolla, S. Coelli, R. Barbieri, A. Pedrocchi, and A. M. Bianchi, “EEG Analysis During Active and Assisted Repetitive Movements: Evidence for Differences in Neural Engagement,” *IEEE Trans. Neural Syst. Rehabil. Eng. Publ. IEEE Eng. Med. Biol. Soc.*, vol. 25, no. 6, pp. 761–771, 2017.
- [9] M. Gandolla *et al.*, “Artificial neural network EMG classifier for functional hand grasp movements prediction,” *J. Int. Med. Res.*, vol. 45, no. 6, pp. 1831–1847, 2017.
- [10] J. V Basmajian, “Biofeedback in rehabilitation: a review of principles and practices.,” *Arch. Phys. Med. Rehabil.*, vol. 62, no. 10, pp. 469–75, Oct. 1981.
- [11] Z. Zhang, H. Wu, W. Wang, and B. Wang, “A smartphone based respiratory biofeedback system,” in *2010 3rd International Conference on Biomedical Engineering and Informatics*, 2010, vol. 2, pp. 717–720.
- [12] O. M. Giggins, U. M. Persson, and B. Caulfield, “Biofeedback in rehabilitation,” *J. NeuroEngineering Rehabil.*, vol. 10, p. 60, Jun. 2013.
- [13] D. J. Smith, S. R. Norris, and J. M. Hogg, “Performance evaluation of swimmers: scientific tools,” *Sports Med. Auckl. NZ*, vol. 32, no. 9, pp. 539–554, 2002.
- [14] J. Komar *et al.*, “Effect of increasing energy cost on arm coordination in elite sprint swimmers,” *Hum. Mov. Sci.*, vol. 31, no. 3, pp. 620–629, Jun. 2012.
- [15] R. H. Sanders, “Kinematics, coordination, variability, and biological noise in the prone flutter kick at different levels of a ‘learn-to-swim’ programme,” *J. Sports Sci.*, vol. 25, no. 2, pp. 213–227, Jan. 2007.
- [16] R. Mooney, G. Corley, A. Godfrey, L. R. Quinlan, and G. ÓLaighin, “Inertial Sensor Technology for Elite Swimming Performance Analysis: A Systematic Review,” *Sensors*, vol. 16, no. 1, Dec. 2015.
- [17] X. Zhu and K. F. Li, “Real-Time Motion Capture: An Overview,” in *2016 10th International Conference on Complex, Intelligent, and Software Intensive Systems (CISIS)*, 2016, pp. 522–525.
- [18] D. Gierlach, A. Gustus, and P. van der Smagt, “Generating marker stars for 6D optical tracking,” in *2012 4th IEEE RAS EMBS International Conference on Biomedical Robotics and Biomechatronics (BioRob)*, 2012, pp. 147–152.
- [19] I. E. Sampe, A. V. N, R. M. T. Latifah, and T. Apriantono, “A study on the effects of lightning and marker color variation to marker detection and tracking accuracy in gait analysis system,”

- in *International Conference on Instrumentation, Communication, Information Technology, and Biomedical Engineering 2009*, 2009, pp. 1–5.
- [20] M. T. K. Tsun, B. T. Lau, H. S. Jo, and S. L. Lau, “A human orientation tracking system using Template Matching and active Infrared marker,” in *2015 International Conference on Smart Sensors and Application (ICSSA)*, 2015, pp. 116–121.
- [21] D. Roetenberg, P. J. Slycke, and P. H. Veltink, “Ambulatory Position and Orientation Tracking Fusing Magnetic and Inertial Sensing,” *IEEE Trans. Biomed. Eng.*, vol. 54, no. 5, pp. 883–890, May 2007.
- [22] H. Dejnabadi, B. M. Jolles, E. Casanova, P. Fua, and K. Aminian, “Estimation and visualization of sagittal kinematics of lower limbs orientation using body-fixed sensors,” *IEEE Trans. Biomed. Eng.*, vol. 53, no. 7, pp. 1385–1393, Jul. 2006.
- [23] M. El-Gohary and J. McNames, “Human Joint Angle Estimation with Inertial Sensors and Validation with A Robot Arm,” *IEEE Trans. Biomed. Eng.*, vol. 62, no. 7, pp. 1759–1767, Jul. 2015.
- [24] H. Fourati, “Heterogeneous Data Fusion Algorithm for Pedestrian Navigation via Foot-Mounted Inertial Measurement Unit and Complementary Filter,” *IEEE Trans. Instrum. Meas.*, vol. 64, no. 1, pp. 221–229, Jan. 2015.
- [25] H. Ahmed and M. Tahir, “Improving the Accuracy of Human Body Orientation Estimation With Wearable IMU Sensors,” *IEEE Trans. Instrum. Meas.*, vol. 66, no. 3, pp. 535–542, Mar. 2017.
- [26] X. Yun, E. R. Bachmann, and R. B. McGhee, “A Simplified Quaternion-Based Algorithm for Orientation Estimation From Earth Gravity and Magnetic Field Measurements,” *IEEE Trans. Instrum. Meas.*, vol. 57, no. 3, pp. 638–650, Mar. 2008.
- [27] G. Wu *et al.*, “ISB recommendation on definitions of joint coordinate system of various joints for the reporting of human joint motion--part I: ankle, hip, and spine. International Society of Biomechanics,” *J. Biomech.*, vol. 35, no. 4, pp. 543–548, Apr. 2002.
- [28] G. Wu *et al.*, “ISB recommendation on definitions of joint coordinate systems of various joints for the reporting of human joint motion--Part II: shoulder, elbow, wrist and hand,” *J. Biomech.*, vol. 38, no. 5, pp. 981–992, May 2005.
- [29] N. Enayati, E. D. Momi, and G. Ferrigno, “A Quaternion-Based Unscented Kalman Filter for Robust Optical/Inertial Motion Tracking in Computer-Assisted Surgery,” *IEEE Trans. Instrum. Meas.*, vol. 64, no. 8, pp. 2291–2301, Aug. 2015.
- [30] Z. Zhang, “Cameras and Inertial/Magnetic Sensor Units Alignment Calibration,” *IEEE Trans. Instrum. Meas.*, vol. 65, no. 6, pp. 1495–1502, Jun. 2016.
- [31] L. S. Vargas-Valencia, A. Elias, E. Rocon, T. Bastos-Filho, and A. Frizera, “An IMU-to-Body Alignment Method Applied to Human Gait Analysis,” *Sensors*, vol. 16, no. 12, Dec. 2016.
- [32] S. Giancola, J. Schneider, P. Wonka, and B. S. Ghanem, “Integration of Absolute Orientation Measurements in the KinectFusion Reconstruction pipeline,” *ArXiv180203980 Cs*, Feb. 2018.
- [33] Z. Zhang and G. Yang, “Calibration of Miniature Inertial and Magnetic Sensor Units for Robust Attitude Estimation,” *IEEE Trans. Instrum. Meas.*, vol. 63, no. 3, pp. 711–718, Mar. 2014.
- [34] B. I. des Poids et Mesures, “Evaluation of measurement data guide for the expression of uncertainty in measurement,” *JCGM*, vol. 100:2008, 2008.
- [35] M. El-Gohary and J. McNames, “Shoulder and Elbow Joint Angle Tracking With Inertial Sensors,” *IEEE Trans. Biomed. Eng.*, vol. 59, no. 9, pp. 2635–2641, Sep. 2012.
- [36] J. Brooke, “SUS-A quick and dirty usability scale,” *Usability Eval. Ind.*, vol. 189, pp. 4–7, 1996.
- [37] E. R. Bachmann, X. Yun, and C. W. Peterson, “An investigation of the effects of magnetic variations on inertial/magnetic orientation sensors,” in *IEEE International Conference on Robotics and Automation, 2004. Proceedings.*

- ICRA '04. 2004*, 2004, vol. 2, p. 1115–1122
Vol.2.
- [38] X.-F. Teng, Y.-T. Zhang, C. C. Y. Poon, and P. Bonato, “Wearable medical systems for p-Health,” *IEEE Rev. Biomed. Eng.*, vol. 1, pp. 62–74, 2008.
- [39] A. Musumeci, G. Pranovi, and S. Masiero, “Patient education and rehabilitation after hip arthroplasty in an Italian spa center: a pilot study on its feasibility,” *Int. J. Biometeorol.*, vol. 62, no. 8, pp. 1489–1496, Aug. 2018.
- [40] S. Ferrante *et al.*, “A biofeedback cycling training to improve locomotion: a case series study based on gait pattern classification of 153 chronic stroke patients,” *J. Neuroengineering Rehabil.*, vol. 8, p. 47, Aug. 2011.
- [41] J. M. Koury, *Aquatic therapy programming: guidelines for orthopedic rehabilitation*. Champaign, IL : Human Kinetics, 1996.
- [42] L. M. Carroll, D. Volpe, M. E. Morris, J. Saunders, and A. M. Clifford, “Aquatic Exercise Therapy for People With Parkinson Disease: A Randomized Controlled Trial,” *Arch. Phys. Med. Rehabil.*, vol. 98, no. 4, pp. 631–638, 2017.
- [43] G. Palamara *et al.*, “Land Plus Aquatic Therapy Versus Land-Based Rehabilitation Alone for the Treatment of Balance Dysfunction in Parkinson Disease: A Randomized Controlled Study With 6-Month Follow-Up,” *Arch. Phys. Med. Rehabil.*, vol. 98, no. 6, pp. 1077–1085, 2017.